A Parametric Model for Saccadic Eye Movement

Weiwei Dai*, Ivan Selesnick*, John-Ross Rizzo†, Janet Rucker†, Todd Hudson†

*Dept. of Electrical and Computer Engineering, Tandon School of Engineering, New York University, Brooklyn, NY
†Dept. of Neurology, School of Medcine, New York University, New York, NY

Abstract—This paper proposes a parametric model for saccadic waveforms. The model has a small number of parameters, yet it effectively simulates a variety of physiologic saccade properties. In particular, the model reproduces the established relationship between peak saccadic angular velocity and saccadic amplitude (i.e., the saccadic main sequence). The proposed saccadic waveform model can be used in the evaluation and validation of methods for quantitative saccade analysis. For example, we use the proposed saccade model to evaluate four well-known saccade detection algorithms. The comparison indicates the most reliable algorithm is one by Nystrom et al. We further use the proposed saccade model to evaluate the standard technique used for the estimation of peak saccadic angular velocity. The evaluation shows the occurrence of systematic errors. We thus suggest that saccadic angular velocity values determined by the standard technique (low-pass differentiation) should be interpreted and used with caution.

Index Terms—saccade, parametric model, main sequence.

I. INTRODUCTION

Saccades are brief human eye movements that continually redirect our line of sight to objects of interest throughout daily life [21]. Difficulties in executing eye movements are among the first symptoms of some neurological diseases [25]. Hence, abnormalities in ocular motor function can have significant meaning to clinicians, and they may provide opportunities for more timely diagnosis and treatment. In fact, eye movements are biomarkers of specific diseases and syndromes and can be tracked longitudinally to evaluate the outcomes of specific interventions. Therefore, the quantitative analysis of saccades can aid in the clinical diagnosis, prognosis, and possibly intervention of various neurological conditions.

In this paper, we propose a parametric model for saccade waveforms. During a saccade, the eye rotates from one angle to another as it moves its focus from one object of interest to another. The angle as a function of time (as the eye rotates) exhibits a particular waveform as shown in Fig. 1. Our proposed parametric saccade waveform model approximates this waveform, mimicking the behavior of a natural saccade. The saccade model has five parameters each with distinct meaning. The model can be used to simulate saccade waveforms of different shape and size.

The proposed saccade waveform model conforms to a well-known empirically observed relation between peak saccadic angular velocity and saccadic amplitude. (The amplitude of a saccade is defined as the total angle traversed during the saccade.) It is known that for small saccades the peak angular velocity tends to be linearly proportional to amplitude [4]. For large saccades there is a saturation effect and the peak
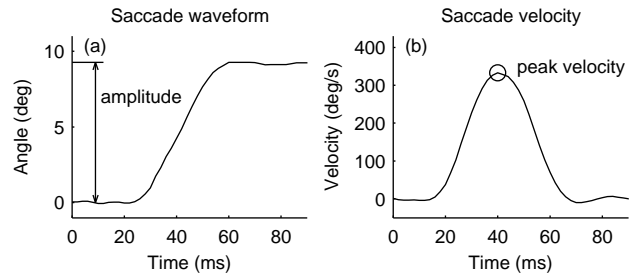

Fig. 1. Saccade (a) angle and (b) angular velocity.

angular velocity reaches a maximum value. This relationship between peak angular velocity and amplitude is known as the saccadic 'main sequence' [4]. It is used as a tool to evaluate saccadic dynamics [7]. Our proposed saccade model not only approximates the waveforms of real saccades but also captures this relationship.

The proposed saccade waveform model simulates saccade waveforms more realistically than models based on simply scaling and translating a fixed waveform. For example, the waveform of a small saccade can be approximated by a sigmoid function or by a Gaussian or Gumbel cumulative distribution function. However, as will be shown in Section III, the proposed model approximates saccade waveforms more accurately, especially larger saccades.

The proposed model can be used to evaluate algorithms for saccade detection. Many saccade detection algorithms have been developed to aid in the quantitative analysis of saccades. But the evaluation of such algorithms is difficult due to disagreement among clinicians as to the interpretation of eye-tracking data. The true timing and dynamics of recorded saccades are not completely known. The use of simulated saccade waveforms provides an objective measure by which to evaluate and compare various saccade detection algorithms. The use of simulated saccades also makes it possible to easily vary the sampling rate and noise contamination conditions. A Matlab program to simulate saccades is available from the author. In Section IV, we compare four saccade detection algorithms using the proposed saccade model.

The proposed model can also be used to evaluate methods to estimate saccadic angular velocity. Abnormally slow saccades are suggestive of diseases involving brainstem saccadic burst neurons [6], [25]; thus, it is quite important in clinical medicine to accurately measure the peak angular velocity of the eye during saccades. Saccadic angular velocity is usually estimated using a low-pass differentiation filter. In Section V,
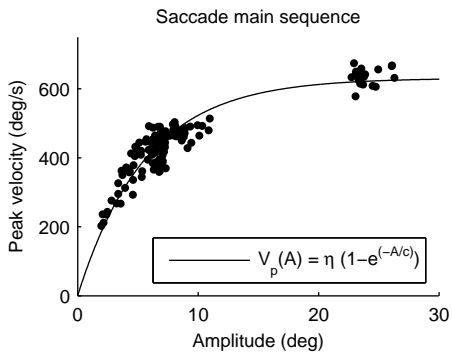
Fig. 2. Peak saccadic angular velocity (V_p) versus saccadic amplitude (A). Each point represent a saccade.

Fig. 3. Saccade model $s(t)$ and its component $f(t)$, $-f(t-\tau)$.

we use the proposed saccade waveform model to show that the estimated peak angular velocity actually depends substantially on the particular filter utilized.

The proposed model is different in purpose and form than previous saccade models. Previous models generally aim to describe the biological-neuronal processes underlying saccades. A purpose of such models is to understand how various parts of the brain work together to control eye movement [2], [17], [20], [26], [29], [36]. Such models take the form of a dynamical system. In contrast, our intention is to model the saccadic waveform itself (not the underlying neural processes) for the purpose of facilitating the evaluation of methods for quantitative analysis of saccades.

II. BACKGROUND

A. Eye Movement Recording Equipment

The search coil is considered the gold standard for eye tracking as it provides high accuracy and high sampling rate recordings. A search coil is a contact-lens-like ring containing coils of thin copper wire [10], [28]. It is placed on the eye of a participant who is siting in a magnetic field during the eye movement recording. However, coil systems are expensive and are no longer widely used. Nowadays, high-speed video-oculographic eye trackers are widely used because they are non-invasive and convenient [27]. Studies suggest that contemporary video tracking now approaches the search coil for measuring eye movements [22], [33].

B. Main Sequence

For small saccades, peak saccadic angular velocity (V_p) tends to be linearly proportional to saccadic amplitude (A); and for large saccades, peak saccadic angular velocity saturates. This phenomenon has been established empirically [4] and can be explained by biological dynamical system models [12], [15], [16], [34]. The data shown in Fig. 2 reflect this behavior. This data consist of eye movements recorded while an individual read lines of alphabetic characters on a page. Small saccades occur when the person looks from one character to another on a line of text; whereas, large saccades occur when the person reaches the end of one line of text and looks to the beginning of the next line. In Fig. 2, each
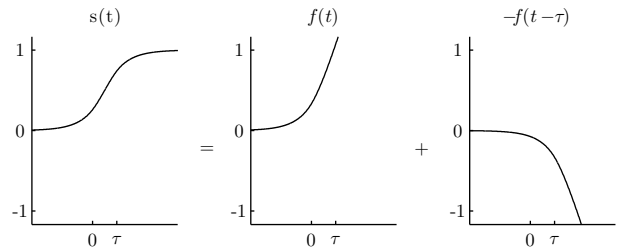
saccade is shown as a point at coordinate (A, V_p) where A is the saccadic amplitude and V_p is the peak saccadic angular velocity. The relationship between V_p and A can be approximated by the exponential function,

$$V_p(A; \eta, c) = \eta\big(1 - e^{-A/c}\big). \tag{1}$$

This equation was proposed by Baloh et al. to permit rapid statistical comparison between subjects with normal and abnormal eye movements and has been shown to be superior to other equations [7]. The parameter η represents the maximum attainable peak angular velocity of any saccade made by the individual. The parameter c determines the proportionality constant between V_p and A for small saccades.

This relationship shown in Fig 2 is known as the saccadic 'main sequence'. The main sequence curve varies from individual to individual, but it is highly reproducible for an individual and cannot be voluntarily altered [9], [14].

C. Saccade Detection Algorithms

A few publications have compared the performance of various saccade detection algorithms; however, the comparisons were conducted using a small data set [1] or simplified tests [19]. Large saccades can be distinguished from other eye movements because they are much faster than other types of eye movements [18], [21]. There are two main classes of saccade detection algorithms: (1) velocity-based and (2) dispersion-based. We briefly review several algorithms here and compare their performance in Section IV.

Velocity-based algorithms analyze the angular velocity of the eye. Given a threshold value, eye movements with angular velocity exceeding the threshold value are classified as saccades. The threshold value must be prescribed with care, because the velocity is adversely affected by noise in the signal. Engbert proposed an algorithm for the detection of microsaccades using an adaptive global threshold [13]. This algorithm estimates the noise of the signal and prescribes a threshold value proportional to it. It works well for both microsaccades and large saccades. Nystrom proposed a more adaptive algorithm, which uses an adaptive global threshold for saccade onset; the threshold value is determined by iteratively estimating noise during fixations [23]. The end of each saccade is determined by a local adaptive threshold value.

Dispersion-based algorithms process directly the angle of the eye and measures its dispersion ('spread'). In contrast to saccades, during fixations the eye moves minimally and
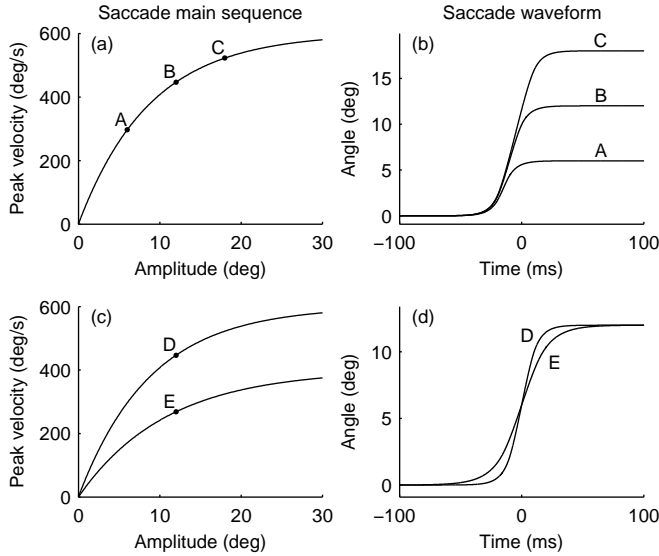
Fig. 4. Simulated saccades. Saccades A, B, C are generated by varying only τ. Saccades D and E have the same amplitude but different peak angular velocity and correspond to different main sequence parameters.

the eye angle is relatively constant [30]. Dispersion-based algorithms classify intervals during which the eye is relatively constant as fixations, and classify other intervals as saccades. These algorithms use a moving window and calculate the dispersion within the window [8], [32].

III. SACCADE MODEL

In this section, we propose a model for saccadic waveforms and describe its parameters. We demonstrate that the proposed model fits physiologic saccades better than other models.

A. Saccade Model Formula

We model a saccadic waveform $s(t)$ as the sum of a soft ramp function $f(t)$ and a shifted negated soft ramp function $-f(t - \tau)$, i.e.,

$$s(t; \eta, c, \tau) = cf(\eta t/c) - cf(\eta(t - \tau)/c) \quad (2)$$

where

$$f(t) = \begin{cases} t + 0.25e^{-2t}, & t \geqslant 0 \\ 0.25e^{2t}, & t \leqslant 0 \end{cases} \quad (3)$$

and η, c, and τ are parameters.

Fig. 3 illustrates how the saccade model $s(t)$ is constructed. Note that the amplitude A of the saccade model $s(t)$ is given by $\eta\tau$,

$$A = \lim_{t \to \infty} s(t) - \lim_{t \to -\infty} s(t) \quad (4)$$
$$= \eta t - \eta(t - \tau) \quad (5)$$
$$= \eta\tau. \quad (6)$$

Observe that the peak angular velocity (V_p) of the saccade model $s(t)$ agrees with formula (1) which relates V_p and A.
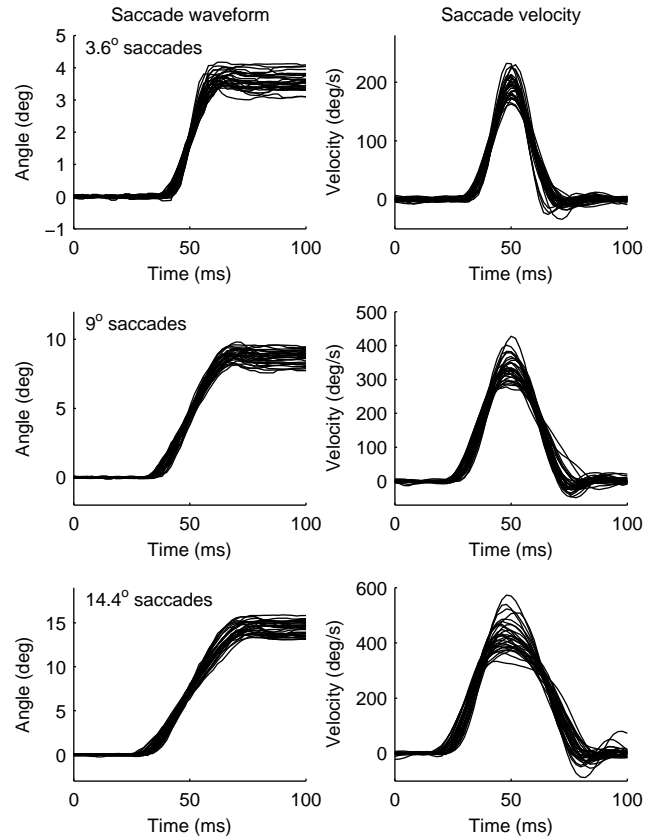

Fig. 5. Waveforms of saccades to targets at $3.6°$, $9°$ and $14.4°$.

Using (2), (3), and (6), we have

$$V_p = s'(\tau/2) \quad (7)$$
$$= \eta f'(\eta\tau/2c) - \eta f'(-\eta\tau/2c) \quad (8)$$
$$= \eta(1 - e^{-A/c}). \quad (9)$$

In (7), we used the fact that the maximum value of $s'(t)$ occurs at $t = \tau/2$. It can be seen in (9) that parameters η and c determine the main sequence equation (1).

B. Saccade Model Parameters

We incorporate two more parameters, t_0 and s_0, to specify the saccade onset time and initial saccadic angle,

$$S(t; \eta, c, \tau, t_0, s_0) = s(t - t_0; \eta, c, \tau) + s_0. \quad (10)$$

The five parameters η, c, τ, t_0, s_0 of the proposed model determine the shape, amplitude, onset time, and initial angle of the simulated saccade.

From (9), the parameters η and c determine the relationship between amplitude A and peak angular velocity V_p of a simulated saccade. The parameter τ thus determines a point on the main sequence curve (1) characterizing the saccade. Hence, τ determines both the amplitude A and peak angular velocity V_p of a simulated saccade $s(t)$ in accordance with the main sequence relation (1). As shown in Figs. 4(a) and 4(b), small, medium and large saccades can be simulated by
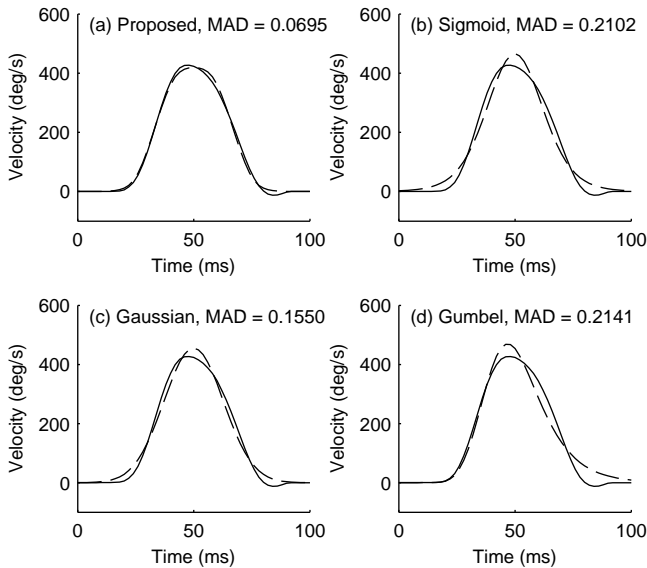
3

Fig. 6. Average angular velocity waveform of $14.4°$ saccades (solid line) fitted by various models (dashed lines). The proposed model fits the saccade better than other models.

TABLE I
FITTING ERROR BETWEEN SACCADE MODELS AND DATA

Saccade amplitude	Mean Absolute Deviation			
	Proposed	Sigmoid	Gaussian	Gumbel
$3.6°$	0.0178	0.0286	0.0195	0.0450
$9°$	0.0400	0.1118	0.0806	0.1401
$14.4°$	0.0695	0.2102	0.1550	0.2141

varying only τ. These simulated saccades lie on a single main sequence curve.

Parameters η, c and τ together determine the shape of the simulated saccade waveform. It is beneficial that the proposed model can simulate saccades conforming to a prescribed $V_p(A)$ relationship, because the main sequence curve is a practical diagnostic tool to distinguish slow saccades from normal saccades. As shown in Figs. 4(c) and 4(d), the proposed model can simulate saccades that have the same amplitude, but correspond to different main sequence relations.

C. Saccade Model Verification

We demonstrate that the proposed model can well approximate physiologic saccades. We acquire a dataset of eye movements of 24 healthy adults making eye movements as quickly as possible to targets that are illuminated to the right and left of a fixation cue on a computer screen. We subsequently detect saccades with an angular velocity threshold ($30°/$s) and extract saccades with amplitudes similar to that of the target amplitudes [24]. Thirty saccades to targets at $3.6°$, $9°$, $14.4°$ are selected. The saccade waveforms are shown in Fig. 5, where they have been mutually aligned. We fit the proposed model to the averaged saccade waveforms (using `fitnlm` in Matlab), as illustrated in Fig. 6(a).

Meanwhile, other functions such as the sigmoid, and Gaussian or Gumbel cumulative distribution function, can also be
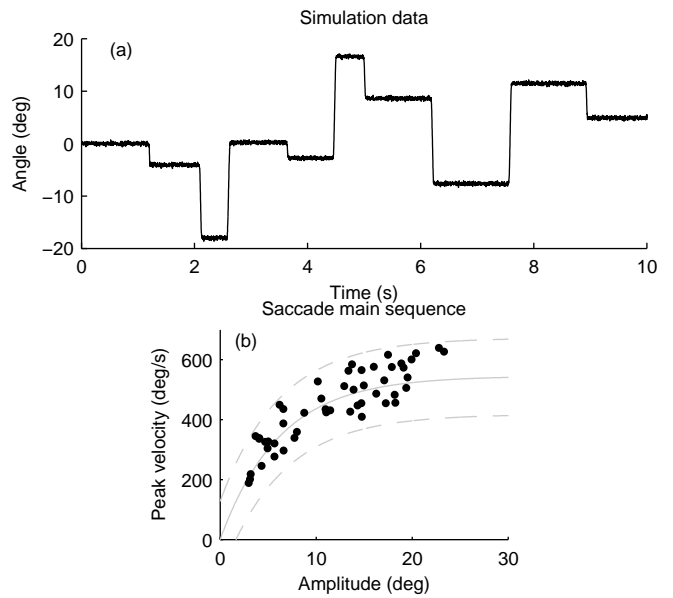

Fig. 7. Simulation data generated by the proposed models

used to model saccade waveforms. Therefore, for comparison, we scale these functions to model saccades,

$$\text{sigmoid}(t) = \frac{a}{1 + e^{-(t-t_0)/b}} + s_0 \qquad (11)$$

$$\text{Gaussian}(t) = \frac{a}{2}\left(1 + \text{erf}\left(\frac{t - t_0}{\sqrt{2}b}\right)\right) + s_0 \qquad (12)$$

$$\text{Gumbel}(t) = ae^{-e^{-(t-t_0)/b}} + s_0 \qquad (13)$$

where a and b are amplitude and temporal scaling parameters.

All models can fit small-amplitude saccades well. However, as shown in Fig. 6, the proposed saccade model fits large-amplitude saccades more accurately than other saccade models. To quantify the fitting error between real and simulated saccade waveforms, we use the mean absolute deviation (MAD), which we report in Table I. The three considered models (11) (12) (13) do not take into account the fact that large-amplitude and small-amplitude saccades have different shapes as reflected by the $V_p(A)$ relation (1) [V_p plateaus at large saccadic amplitudes].

IV. SACCADE DETECTION ALGORITHMS

The proposed parametric saccade waveform model can be used to evaluate saccade detection algorithms. The model allows the simulations of saccades that conform to a designated $V_p(A)$ relationship ('main sequence') which can vary from one individual to another individual, resulting in unique person-specific main sequence curves. With a large dataset, we hence have a range of parameters in the main sequence equation (η and c). We can easily simulate many saccades of different size and shape, with arbitrary inter-saccadic intervals as shown in Fig. 7. This is a simulation (at 500 samples/second) of one person making saccades to the left and right, with the simulated saccades being normative (as shown in Fig. 7).
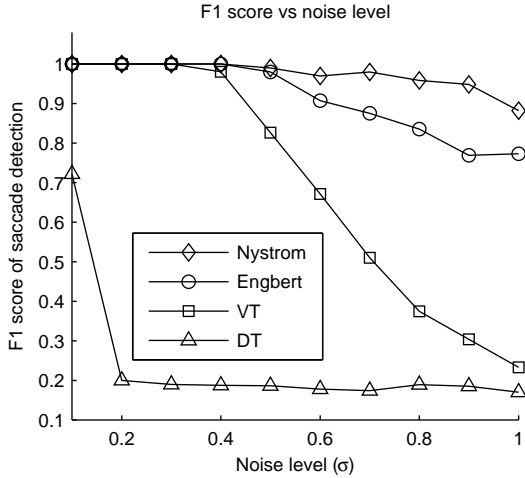
Fig. 8. Evaluation of four saccade detection algorithms.

We use simulated saccades to evaluate four common saccade detection algorithms. Eye movement data from video tracking systems tends to be noisy due to the difficulty of continuously and accurately identifying the pupil and cornea reflection [24]. Therefore, we add white Gaussian noise to simulate pervasive measurement noise to test the robustness of the saccade detection algorithms. To measure and compare the performance of the saccade detection algorithms, we calculate F1 scores as in [35]; see Fig. 8.

$$\text{F1 score} = 2 \frac{\text{Precsion} \cdot \text{Recall}}{\text{Precision} + \text{Recall}} \tag{14}$$

$$\text{Precision} = \frac{\text{True Positive}}{\text{True Positive} + \text{False Positive}} \tag{15}$$

$$\text{Recall} = \frac{\text{True Positive}}{\text{True Positive} + \text{False Negative}} \tag{16}$$

The four saccade detection algorithms exhibit markedly different performance profiles, especially in the presence of noise. The dispersion threshold algorithm (DT) is the least accurate because it is designed for fixation and regards anything else as a saccade [30]. Simple velocity threshold (VT) algorithms and adaptive velocity threshold (Engbert, Nystrom) algorithms perform similarly when the noise is small [13], [23]. At higher noise levels, simple velocity threshold results in many false positive detections. The global adaptive velocity threshold algorithm (Engbert) also results in false negatives (i.e., non-detected saccades). Therefore, in terms of the F1 score, the Nystrom algorithm appears to be the most robust of the four algorithms.

V. Saccade Peak Velocity Estimation

Peak saccadic angular velocity can be used as a biomarker of brainstem burst neuron disease and a sign of fatigue [11]. But accurately measuring saccadic angular velocity is difficult because of noise and the short duration of saccades. Differentiation (to calculate velocity) is vulnerable to noise.
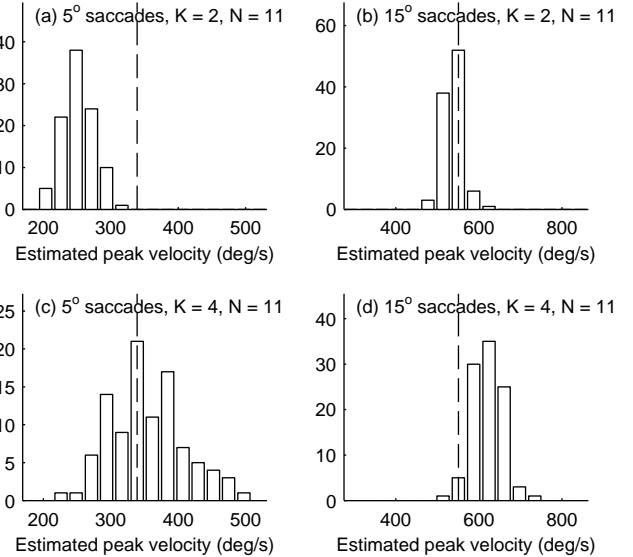

Fig. 9. Histogram of peak saccadic angular velocity estimated using SG filters of different polynomial order K. The dashed line indicates the true peak saccadic angular velocity.

Pure differentiation amplifies noise. Hence, differentiation is typically performed in conjunction with low-pass filtering to avoid noise amplification. But low-pass filtering smooths data and leads to an underestimation of peak angular velocity.

We use simulate saccades to study the accuracy of peak angular velocity as estimated using a low-pass differentiation filter. Here, we use the proposed model to simulate one hundred $5°$ and $15°$ saccades (at 500 samples/second) and add white Gaussian noise $\mathcal{N}(0, 0.5)$ to the simulated saccades. We use the Savitzky-Golay (SG) low-pass differentiation filter [31] (`sgolay` in Matlab) to estimate the peak saccadic angular velocity because this filter is often used for eye movement analysis. Fig. 9 shows the results.

The accuracy of the estimated peak saccadic angular velocity depends on the particular low-pass differentiation filter [5]. The SG differentiator with impulse response of length $N = 11$ and polynomial order $K = 2$, severely underestimates peak angular velocity of small-amplitude saccades, as shown in Fig. 9(a), and slightly underestimates peak angular velocity of large-amplitude saccades, as shown in Fig. 9(b). The SG differentiator with polynomial order $K = 4$ (corresponding to a higher cut-off frequency) estimates peak angular velocity of small saccades more accurately, as shown in Fig. 9(c). However, this filter overestimates the peak angular velocity of large-amplitude saccades, as shown in Fig. 9(d). This suggests different filters should be used for saccades of different amplitude to more accurately estimate peak angular velocity.

VI. Conclusion

In this paper, we propose a parametric model for saccadic waveform simulation, that fits saccades more accurately than scaled-sigmoidal models. The proposed model conforms to the established relation (1) between peak saccadic angular velocity and saccadic amplitude. The proposed model is simple, yet it

approximates a variety of saccadic behaviors that recapitulate normative physiology.

We demonstrate the use of the proposed saccade model to evaluate basic methods for quantitative saccade analysis. Using the model, we compare the performance of four saccade detection algorithms and identified the algorithm by Nystrom et al. as being the most robust to noise. We also use the model to investigate the statistical accuracy of peak saccadic angular velocity as estimated by the standard technique (low-pass differentiation). We find that a prescribed low-pass differentiation filter may systematically underestimate or overestimate the peak saccadic angular velocity. It follows that one should exercise caution in the interpretation and use of peak saccadic angular velocities as estimated by the standard technique.

The saccade waveform model presented in this paper assumes the angular velocity profile is symmetric. While small-amplitude saccades are approximately symmetric, large-amplitude saccades tend to be skewed (non-symmetric). Hence, it will be of interest in future work to generalize the proposed model to the non-symmetric case. That being said, normal human saccadic eye movements are seldom larger than 15 degrees [3]. As the proposed model is satisfactory for saccades of this size (cf. Fig. 6), it should have practical value as presented.

REFERENCES

[1] R. Andersson, L. Larsson, K. Holmqvist, M. Stridh, and M. Nyström. One algorithm to rule them all? An evaluation and discussion of ten eye movement event-detection algorithms. *Behavior Research Methods*, pages 1–22, 2016.

[2] K. Arai, S. Das, E. L. Keller, and E. Aiyoshi. A distributed model of the saccade system: simulations of temporally perturbed saccades using position and velocity feedback. *Neural Networks*, 12(10):1359–1375, 1999.

[3] A. T. Bahill, D. Adler, and L. Stark. Most naturally occurring human saccades have magnitudes of 15 degrees or less. *Investigative Ophthalmology & Visual Science*, 14(6):468–469, 1975.

[4] A. T. Bahill, M. R. Clark, and L. Stark. The main sequence, a tool for studying human eye movements. *Mathematical Biosciences*, 24(3):191–204, 1975.

[5] A. T. Bahill, J. S. Kallman, and J. E. Lieberman. Frequency limitations of the two-point central difference differentiation algorithm. *Biological Cybernetics*, 45(1):1–4, 1982.

[6] R. W. Baloh, H. R. Konrad, A. W. Sills, and V. Honrubia. The saccade velocity test. *Neurology*, 25(11):1071–1071, 1975.

[7] R. W. Baloh, A. W. Sills, W. E. Kumley, and V. Honrubia. Quantitative measurement of saccade amplitude, duration, and velocity. *Neurology*, 25(11):1065–1065, 1975.

[8] P. Blignaut. Fixation identification: The optimum threshold for a dispersion algorithm. *Attention, Perception, & Psychophysics*, 71(4):881–895, 2009.

[9] R. J. Brockhurst and K. S. Lion. Analysis of ocular movements by means of an electrical method. *American Medical Association Archives of Ophthalmology*, 46(3):311–314, 1951.

[10] H. Collewijn, C. J. Erkelens, and R. M. Steinman. Binocular coordination of human horizontal saccadic eye movements. *The Journal of Physiology*, 404:157, 1988.

[11] L. L. Di Stasi, R. Renner, A. Catena, J. J. Cañas, B. M. Velichkovsky, and S. Pannasch. Towards a driver fatigue test based on the saccadic main sequence: A partial validation by subjective report data. *Transportation Research Part C: Emerging Technologies*, 21(1):122–133, 2012.

[12] J. D. Enderle and J. W. Wolfe. Time-optimal control of saccadic eye movements. *IEEE Trans. Biomedical Engineering*, (1):43–55, 1987.

[13] R. Engbert and R. Kliegl. Microsaccades uncover the orientation of covert attention. *Vision Research*, 43(9):1035–1045, 2003.

[14] P. F. Gangemi, A. Messori, S. Baldini, A. Parigi, S. Massi, and G. Zaccara. Comparison of two nonlinear models for fitting saccadic eye movement data. *Computer Methods and Programs in Biomedicine*, 34(4):291–297, 1991.

[15] C. M. Harris and D. M. Wolpert. The main sequence of saccades optimizes speed-accuracy trade-off. *Biological Cybernetics*, 95(1):21–29, 2006.

[16] M. R. Harwood, L. E. Mezey, and C. M. Harris. The spectral main sequence of human saccades. *The Journal of Neuroscience*, 19(20):9098–9106, 1999.

[17] F. K. Hsu, A. T. Bahill, and L. Stark. Parametric sensitivity analysis of a homeomorphic model for saccadic and vergence eye movements. *Computer Programs in Biomedicine*, 6(2):108–116, 1976.

[18] P. Inchingolo and M. Spanio. On the identification and analysis of saccadic eye movements-a quantitative study of the processing procedures. *IEEE Trans. Biomedical Engineering*, (9):683–695, 1985.

[19] O. V. Komogortsev, D. V. Gobert, S. Jayarathna, D. H. Koh, and S. M. Gowda. Standardization of automated analyses of oculomotor fixation and saccadic behaviors. *IEEE Trans. Biomedical Engineering*, 57(11):2635–2645, 2010.

[20] P. Lefèvre, C. Quaia, and L. M. Optican. Distributed model of control of saccades by superior colliculus and cerebellum. *Neural Networks*, 11(7):1175–1190, 1998.

[21] R. J. Leigh and D. S. Zee. *The neurology of eye movements*. Oxford University Press, 2015.

[22] M. B. McCamy, J. Otero-Millan, R. J. Leigh, S. A. King, R. M. Schneider, S. L. Macknik, and S. Martinez-Conde. Simultaneous recordings of human microsaccades and drifts with a contemporary video eye tracker and the search coil technique. *PLoS One*, 10(6):e0128428, 2015.

[23] M. Nyström and K. Holmqvist. An adaptive algorithm for fixation, saccade, and glissade detection in eyetracking data. *Behavior Research Methods*, 42(1):188–204, 2010.

[24] M. Nyström, I. Hooge, and R. Andersson. Pupil size influences the eye-tracker signal during saccades. *Vision Research*, 121:95–103, 2016.

[25] S. Ramat, R. J. Leigh, D. S. Zee, and L. M. Optican. What clinical disorders tell us about the neural control of saccadic eye movements. *Brain*, 130(1):10–35, 2007.

[26] S. Ramat, R. J. Leigh, D. S. Zee, A. G. Shaikh, and L. M. Optican. Applying saccade models to account for oscillations. *Progress in Brain Research*, 171:123–130, 2008.

[27] J.-R. Rizzo, T. E. Hudson, W.-W. Dai, N. Desai, A. Yousefi, D. Palsana, I. Selesnick, L. J. Balcer, S. L. Galetta, and J. C. Rucker. Objectifying eye movements during rapid number naming: Methodology for assessment of normative data for the King-Devick test. *Journal of the Neurological Sciences*, 2016.

[28] D. A. Robinson. A method of measuring eye movemnent using a scieral search coil in a magnetic field. *IEEE Trans. Bio-medical Electronics*, 10(4):137–145, 1963.

[29] D. A. Robinson. Models of the saccadic eye movement control system. *Kybernetik*, 14(2):71–83, 1973.

[30] D. D. Salvucci and J. H. Goldberg. Identifying fixations and saccades in eye-tracking protocols. In *Proceedings of the 2000 Symposium on Eye Tracking Research & Applications*, pages 71–78. ACM, 2000.

[31] A. Savitzky and M. J. E. Golay. Smoothing and differentiation of data by simplified least squares procedures. *Analytical Chemistry*, 36(8):1627–1639, 1964.

[32] F. Shic, K. Chawarska, and B. Scassellati. The amorphous fixation measure revisited: With applications to autism. In *30th Annual Meeting of the Cognitive Science Society*, pages 1–6, 2008.

[33] J. N. Van der Geest and M. A. Frens. Recording eye movements with video-oculography and scleral search coils: a direct comparison of two methods. *Journal of Neuroscience Methods*, 114(2):185–195, 2002.

[34] A. J. Van Opstal and H. Kappen. A two-dimensional ensemble coding model for spatial-temporal transformation of saccades in monkey superior colliculus. *Network: Computation in Neural Systems*, 4(1):19–38, 1993.

[35] S. C. Warby, S. L. Wendt, P. Welinder, E. G. S. Munk, O. Carrillo, H. B. D. Sorensen, P. Jennum, P. E. Peppard, P. Perona, and E. Mignot. Sleep-spindle detection: crowdsourcing and evaluating performance of experts, non-experts and automated methods. *Nature methods*, 11(4):385–392, 2014.

[36] D. S. Zee, L. M. Optican, J. D. Cook, D. A. Robinson, and W. K. Engel. Slow saccades in spinocerebellar degeneration. *Archives of Neurology*, 33(4):243–251, 1976.